BTD65-143

ATLAS/CENTAUR FLIGHT

PERFORMANCE RESERVE

MONTE CARLO ANALYSIS

AC-7

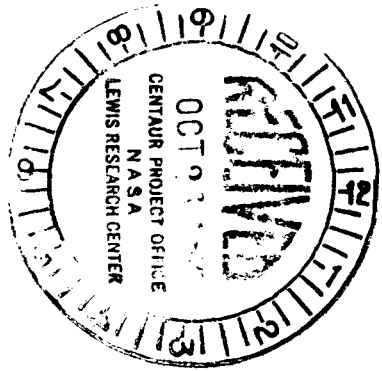GD|C-BTD65-143

17 September 1965

CONTRACT NAS3-3232

GPO PRICE $ _____

CFSTI PRICE(S) $ _____

Hard copy (HC) $3.00

Microfiche (MF) 1.50

ff 653 July 65

GENERAL DYNAMICS | CONVAIR

OCT 26 1965

FOREWORD

This report presents a technique for rapidly evaluating

Flight Performance Reserve requirements for the Centaur

vehicle in combination with an arbitrary booster config-

uration. Application of the model is made and results are

presented for the Atlas/Centaur, AC-7, configuration.
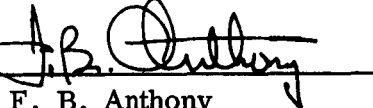
This report supersedes and completely replaces all pre-

vious Atlas/Centaur Flight Performance Reserve studies.

The study was conducted under provisions of Contract

NAS3-3232.

Prepared by _____
        J. F. Ingber
        Senior Research Engineer

Approved by _____
        F. B. Anthony
        Research Group Engineer
        Aeroballistics

Approved by _____
        R. S. Wentink
        Assistant Chief Engineer
        Design Analysis - Centaur

A112

OCT 26 1965

SUMMARY

19446

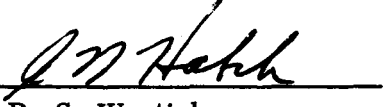This report first discusses a Monte Carlo method which has been developed for the computation of Flight Performance Reserve (FPR) requirements for a Booster X/ Centaur configuration. Second, the results of an application of the model to the Atlas/ Centaur AC-7 configuration are presented.

Toward the end of this study, an operating characteristic of the Centaur Propellant Utilization (PU) System known as "PU End Effect" was identified. Since, however, a significant amount of effort had been expended prior to the identification of this characteristic, and since it is likely that "PU End Effect" logic will be modified, it was deemed desirable to publish the report proper without "PU End Effect" and to include an appendix treating this subject separately.

At the time this study was initiated, the major unknown variable of the problem was PU system accuracy. Thus the results are presented parametrically as a function of this variable. Present PU control system error analysis indicates a system uncertainty of approximately ± 25 pounds equivalent LH_2. Results for this condition are summarized below for direct ascent Surveyor missions. Note the 30 pound loss in payload capability due to PU System "End Effect." *auehu*

CASE	CONDITION	PU ACCURACY LBS - LH_2	LH2 BIAS	FPR	NET PAYLOAD GAIN
0	Old Analysis (Ref. 4)	± 90	60	180	0
1	Current Analysis Without End Effect	± 25	9	145	86
2	Current Analysis With End Effect	± 25	22	162	56

Variations of these values across a launch window are presented. Also, the functional relationships between PU accuracy, PU bias setting and associated FPR are derived.

TABLE OF CONTENTS

LIST OF ILLUSTRATIONS

LIST OF TABLES

SECTION 1

INTRODUCTION

A Monte Carlo method is essentially a sampling method for studying an artificial stochastic model of a physical or mathematical process. Systems of equations whose solutions are not readily obtainable by standard numerical techniques often may be handled by a stochastic process involving parameters that satisfy the equations. Often a judicious application of the physical model is made circumventing the functional equations entirely.

The evaluation of Flight Performance Reserve (FPR), which is the fuel required to be held in reserve to provide for mission success under non-nominal flight operation, may be handled effectively by the above technique. The functional equations which describe the fuel reserve requirements are simply the multi-degree-of-freedom equations of motion for a powered vehicle. The cost of such a direct approach quickly becomes prohibitive for more than a few parameters. Precision numerical solutions to such equations are generally limited to near-nominal conditions for all variables.

The physical model is briefly vehicle performance, measured by either velocity or by burn-out weight at specified injection conditions, which is somewhat loosely related to a number of vehicle parameters.

In the former case, performance is given by

$$V = \sum_{i=1}^{n} \left\{ I_i \, g \ln (MR_i) - M_i - D_i - G_i \right\} . \tag{1}$$

where

n = the number of intervals from lift-off to injection.

I_i = specific impulse in the ith interval.

MR_i = vehicle mass ratio in the ith interval.

M_i = thrust misalignment loss in the ith interval.

D_i = drag loss in the ith interval.

G_i = gravity loss in the ith interval.

In the latter case, performance expressed as burn-out weight (W_{BO}) is

$$W_{BO} = P(\alpha_1, \alpha_2, \cdots, \alpha_n) \tag{2}$$

where the form of the function P is arbitrary and the α's are vehicle-related parameters that influence performance capability.

Equations 1 and 2 both yield the same result consistent with precision numerical techniques mentioned before. However, the simple form of Equation 2 along with the direct correspondence between the α's and FPR make it the basis for this study.

Historically, FPR has been computed by an RSS technique which assumes independence of variables. That is, given a set of parameters p_1, p_2, $\cdots$ p_n and their associated independent changes in the vehicle's performance δp_1, δp_2, $\cdots$ δp_n, then

$$(3\sigma)\ FPR = \sqrt{\delta p_1^2 + \delta p_2^2 + \cdots + \delta p_n^2} \tag{3}$$

which ignores any covariant contribution to the calculation. Of the parameters traditionally used to determine FPR (those which contribute significantly to performance changes) many are clearly dependent. This apparent contradiction, coupled with the desire for a flexible tool to quickly evaluate the contributions of parameter variations to FPR provided the stimulus for the present effort.

SECTION 2

BASIC EQUATIONS

The basic equations for this analysis are derived from a performance function P which is configuration- and mission-independent.

Let

$$P = P(\alpha_1, \alpha_2, \cdots, \alpha_n) \tag{4}$$

represent some vehicle's performance as a function of the n variables α_i. These are arbitrary but, in total, should be comprehensive in depicting any significant performance changes. Equation 4, then, is an explicit representation of performance measured as injection weight into a specified orbit.

Therefore,

$$dP = \frac{\partial P}{\partial \alpha_1} d\alpha_1 + \frac{\partial P}{\partial \alpha_2} d\alpha_2 + \cdots + \frac{\partial P}{\partial \alpha_n} d\alpha_n = \sum_{i=1}^{n} \frac{\partial P}{\partial \alpha_i} d\alpha_i \tag{5}$$

which holds whether or not the α_i's are independent.

Generally, Equation 5 is not evaluated directly since there may exist r relations of the form

$$\Phi(\alpha_1, \alpha_2, \cdots, \alpha_k) = 0 \tag{6}$$

correlating the variables considered.

Theoretically, it is possible to solve for the r α's in terms of the other n-r α's so that

$$dP = \sum_{i=1}^{n-r} \frac{\partial P^1}{\partial \alpha_i} d\alpha_i \tag{7}$$

where the function P^1 contains only independent variables. The difficulty associated with a concise formulation of the functions (Equation 6) is evident, necessitating a simplified approach.

The technique used to evaluate changes in vehicle performance, dP, corresponding to variations in the parameter values, dα, is to use Equation 5 with the selection procedure for the dα_i modified to account for interdependence of the α's. (Otherwise, Equation 7 could be used directly with the selection of dα_i completely random.) Also, the function P is approximated by a related function f.

Sections 3 and 4 treat the generation of these quantities.

The analysis, then, involves the computation of the quantities

$$\sum^{\ell} \Delta P = \sum^{\ell} \sum_{i=1}^{n} \frac{\partial f}{\partial \alpha_i} d\alpha_i \qquad (8)$$

and

$$\sum^{\ell} \Delta P^2 = \sum^{\ell} \left\{ \sum_{i=1}^{n} \frac{\partial f}{\partial \alpha_i} d\alpha_i \right\}^2 \qquad (9)$$

where ℓ is the number of iterations required for a given confidence in the statistics.

It can be shown that the parent distribution associated with the above method will be approximately normal regardless of the individual variable distributions. Therefore, the mean m and standard deviation s of the vehicle's performance subjected to the ranges of the α variations are given directly by

$$m = \ell^{-1} \sum \Delta P \qquad (10)$$

and

$$s = \sqrt{\ell^{-1} \sum \Delta P^2 - m^2} \qquad (11)$$

4

The associated standard errors are

$$\sigma^2(m) = s^2 \ell^{-1} \tag{12}$$

and

$$\sigma^2(s) = s^2 (2\ell)^{-1} \tag{13}$$

where the parent variance is estimated from the sample variance.

SECTION 3

PERFORMANCE PARTIALS

The performance partials are generated by the use of a precision two-body powered-flight computer simulation, Reference 1.

Each variable is assumed to have a specified range of variation. Usually, the range is given as a maximum and minimum dispersion about some nominal value.[*]

Then, selected values within the range of each of the variables in Equation 4 are input as perturbations to the above computer simulation while keeping the other variables constant. The procedure is repeated for each of the n α's.

The fact that some of the α variations may not be directly controllable by input quantities to the computer program accounts for the slight discrepancy between the function P in Equation 4 and the function f in Equations 8 and 9. This is the case, for instance, with some of the variables in the Atlas propulsion block. Generally, the functions P and f may be considered similar for the generation of performance partials.

The outlined procedure will yield a performance function across the range of each of the variables considered. Then, by differencing the nominal and dispersed performance, a derivative function over the range is established.

Clearly, n parameters will produce n derivative functions which may then be interpolated depending on the particular dα selected.

Experience indicates that a linear function is an acceptable approximation to the derivative, for most parameters, when computing FPR.

---

[*] These are often referred to as 3σ values. In practice, however, the conservatism usually attached to such quoted values relegates them to an extremum category.

SECTION 4

PERFORMANCE PARAMETER VARIATIONS

When applicable, parameter variations are selected by a random process from pre-established distribution functions. Generally, these distributions will assume a Gaussian form (often for lack of a more descriptive function). Any distribution may, nevertheless, be specified for any of the n parameters considered.

Let $R(\lambda, \nu)$ be a random variate from some distribution with parameters λ, ν. For a Gaussian distribution (the form assumed for R unless otherwise noted), λ and ν are the mean and standard deviation respectively.

Also, let σ_i be the standard deviation of the ith parameter's variation. Similarly, σ_{i_j} is the standard deviation of the jth variable associated with the ith parameter.

Table 1 presents the methods presently used in determining the $d\alpha$'s. Nominal thrust and specific impulse at given mixture ratios are given in Figures 1 and 2 respectively. Tables 2 and 3 give pressure, density, temperature, and wind variations.

Table 1. Selection Process for Parameter Dispersions

$d\alpha$	PARAMETER	SELECTION PROCESS
	COMPONENT WEIGHT DATA (DRY)	
$d\alpha_1$	Booster	$d\alpha_1 = R(0, \sigma_1)$
$d\alpha_2$	Sustainer and Inter-stage Adapter	$d\alpha_2 = R(0, \sigma_{2_1}) + R(0, \sigma_{2_2})$
$d\alpha_3$	Centaur	$d\alpha_3 = R(0, \sigma_3)$
$d\alpha_4$	Nose Fairing	$d\alpha_4 = R(0, \sigma_4)$
$d\alpha_5$	Insulation Panels	$d\alpha_5 = R(0, \sigma_5)$

Table 1. Selection Process for Parameter Dispersions, Contd

$d\alpha$	PARAMETER	SELECTION PROCESS
	BOOSTER FLIGHT EXPENDABLES	
$d\alpha_6$	Fuel Weight	
	Fuel Density	$BFDD = R(0, \sigma_{6_1})$ $d\alpha_{6_1} = BFDD \cdot NFTV$
	Probe Location	$d\alpha_{6_2} = R(0, \sigma_{6_2})$
	Surface Level Variation	$d\alpha_{6_3} = R(0, \sigma_{6_3})$
	Tank Pressure	$d\alpha_{6_4} = R(0, \sigma_{6_4})$
	Tank Volume	$d\alpha_{6_5} = R(0, \sigma_{6_5})$
	Tanking Level	$d\alpha_{6_6} = R(0, \sigma_{6_6})$
	Ground Expended	$d\alpha_{6_7} = R(0, \sigma_{6_7})$
	Sustainer Thrust Decay	$d\alpha_{6_8} = R(0, \sigma_{6_8})$
		Then, $$d\alpha_6 = \left\{ (NBFD + BFDD) \sum_{i=1}^{6} d\alpha_{6_i} \right\} + d\alpha_7 + d\alpha_8$$
$d\alpha_7$	Fuel Density	$d\alpha_7 = BFDD$
$d\alpha_8$	Oxidizer Weight	
	Oxidizer Density	$BODD = R(0, \sigma_{8_1})$ $d\alpha_{8_1} = BODD \times NOTV$
	Sensor Location	$d\alpha_{8_2} = R(0, \sigma_{8_2})$
	Surface Level Variation	$d\alpha_{8_3} = R(0, \sigma_{8_3})$
	Tank Pressure	$d\alpha_{8_4} = R(0, \sigma_{8_4})$
	Tank Volume	$d\alpha_{8_5} = R(0, \sigma_{8_5})$

Table 1. Selection Process for Parameter Dispersions, Contd

$d\alpha$	PARAMETER	SELECTION PROCESS
	Tanking Level	$d\alpha_{8_6} = R(0, \sigma_{8_6})$
	Ground Expended	$d\alpha_{8_7} = R(0, \sigma_{8_7})$
	Thrust Decay	$d\alpha_{8_8} = R(0, \sigma_{8_8})$
		Then, $$d\alpha_8 = \left\{ (NBOD + BODD) \sum_{i=1}^{6} d\alpha_{8_i} \right\} + d\alpha_{8_7} + d\alpha_{8_8}$$
$d\alpha_9$	Oxidizer Density	$d\alpha_9 = BODD$

<div align="center">

CENTAUR FLIGHT EXPENDABLES

</div>

$d\alpha$	PARAMETER	SELECTION PROCESS
$d\alpha_{10}$	Fuel Weight	
	Sensor Sensitivity	$d\alpha_{10_1} = R(0, \sigma_{10_1})$
	Sensor Location	$d\alpha_{10_2} = R(0, \sigma_{10_2})$
	Surface Variations	$d\alpha_{10_3} = R(0, \sigma_{10_3})$
	Density	$CFDD = R(0, \sigma_{10_4}) \cdot NLH2D$ $d\alpha_{10_4} = CFDD \times NLH2V$
	Tank Volume	$d\alpha_{10_5} = R(0, \sigma_{10_5})(NLH2D + CFDD)$
	Tank Ullage	$d\alpha_{10_6} = -R(MFUV, \sigma_{10_6}) \times (NLH2D + CFDD)$
		Then, $$d\alpha_{10} = \sum_{i=1}^{6} d\alpha_{10_i}$$
$d\alpha_{11}$	Oxidizer Weight	
	Sensor Sensitivity	$d\alpha_{11_1} = R(0, \sigma_{11_1})$
	Sensor Location	$d\alpha_{11_2} = R(0, \sigma_{11_2})$
	Surface Variations	$d\alpha_{11_3} = R(0, \sigma_{11_3})$

Table 1. Selection Process for Parameter Dispersions, Contd

$d\alpha$	PARAMETER	SELECTION PROCESS
$d\alpha_{12}$	Density	$CODD = R(0, \sigma_{11_4}) \times NLO2D$ $d\alpha_{11_4} = CODD \times NLO2V$
	Tank Volume	$d\alpha_{11_5} = R(0, \sigma_{11_5}) \times (NLO2D + CODD)$
	Tank Ullage	$d\alpha_{11_6} = -R(MOUV, \sigma_{11_6}) \times (NLO2D + CFDD)$ Then, $d\alpha_{11} = \sum_{i=1}^{6} d\alpha_{11_i}$
	Booster Jettisoned Residuals	
	Trapped Fuel	$d\alpha_{12_1} = R(0, \sigma_{12_1})$
	Trapped Oxidizer	$d\alpha_{12_2} = R(0, \sigma_{12_2})$
	Lube Oil	$d\alpha_{12_3} = R(0, \sigma_{12_3})$
	Helium	$d\alpha_{12_4} = R(0, \sigma_{12_4})$ Then, $d\alpha_{12} = \sum_{i=1}^{4} d\alpha_{12_i}$
$d\alpha_{13}$	**Sustainer Jettisoned Residuals**	
	Trapped Fuel	$d\alpha_{13_1} = R(0, \sigma_{13_1})$
	Trapped Oxidizer	$d\alpha_{13_2} = R(0, \sigma_{13_2})$
	Lube Oil	$d\alpha_{13_3} = R(0, \sigma_{13_3})$
	Helium	$d\alpha_{13_4} = R(0, \sigma_{13_4})$
	Nitrogen	$d\alpha_{13_5} = R(0, \sigma_{13_5})$
	GO_2 in Tank-Flight	$d\alpha_{13_6} = R(0, \sigma_{13_6})$

Table 1. Selection Process for Parameter Dispersions, Contd

$d\alpha$	PARAMETER	SELECTION PROCESS
$d\alpha_{14}$	GO_2 in Tank-Ground	$d\alpha_{13_7} = R \, (MGO2TG)$
	PU Bias	$d\alpha_{13_8} = R \, (SPUB, \, \sigma_{13_8})$ Then, $d\alpha_{13} = \sum_{i=1}^{8} d\alpha_{13_i}$
	Centaur Jettisoned Residuals	
	Trapped LO_2	$d\alpha_{14_1} = R \, (0, \, \sigma_{14_1})$
	Trapped LH_2	$d\alpha_{14_2} = R \, (0, \, \sigma_{14_2})$
	GO_2 in Tank	$d\alpha_{14_3} = R \, (0, \, \sigma_{14_3})$
	GH_2 in Tank	$d\alpha_{14_4} = R \, (0, \, \sigma_{14_4})$
	H_2O_2 Weight	$d\alpha_{14_5} = R \, (0, \, \sigma_{14_5})$
	Helium	$d\alpha_{14_6} = R \, (0, \, \sigma_{14_6})$
	Ice and Frost	$d\alpha_{14_7} = R \, (0, \, \sigma_{14_7})$
	PU	$d\alpha_{14_8} = R \, (0, \, \sigma_{14_8})$ if $R \geq -CPUB$ (FLAG = 1) otherwise, $d\alpha_{14_8} = -PUSET \, (d\alpha_{14_8} + CPUB) - CPUB$ This method assumes a null mixture ratio after probe uncovery. See Appendix for actual method. Then, $d\alpha_{14} = \sum_{i=1}^{8} d\alpha_{14_i}$

Table 1. Selection Process for Parameter Dispersions, Contd

$d\alpha$	PARAMETER	SELECTION PROCESS
		CENTAUR VENTING
$d\alpha_{15}$	Ground and Inflight LH$_2$	$d\alpha_{15} = R(0, \sigma_{15})$
$d\alpha_{16}$	Ground and Inflight LO$_2$	$d\alpha_{16} = R(0, \sigma_{16})$
$d\alpha_{17}$	Coast	$d\alpha_{17} = R(0, \sigma_{17})$
		BOOSTER PROPULSION
$d\alpha_{18}$	Booster Mixture Ratio	$d\alpha_{18} = R(0, \sigma_{18})$
$d\alpha_{19}$	Booster Thrust	$d\alpha_{19} = T_B(d\alpha_{18}) + R(0, \sigma_{19})$
$d\alpha_{20}$	Booster I$_{sp}$	$d\alpha_{20} = I_B(d\alpha_{18}) + R(0, \sigma_{20})$
$d\alpha_{21}$	Sustainer Mixture Ratio	$d\alpha_{21} = R(0, \sigma_{21})$
$d\alpha_{22}$	Sustainer Thrust	$d\alpha_{22} = T_S(d\alpha_{21}) + R(0, \sigma_{22})$
$d\alpha_{23}$	Sustainer I$_{sp}$	$d\alpha_{23} = I_S(d\alpha_{21}) + R(0, \sigma_{23})$
$d\alpha_{24}$	Vernier Mixture Ratio	$d\alpha_{24} = R(0, \sigma_{24})$
$d\alpha_{25}$	Vernier Thrust	$d\alpha_{25} = T_V(d\alpha_{24}) + R(0, \sigma_{25})$
$d\alpha_{26}$	Vernier I$_{sp}$	$d\alpha_{26} = I_V(d\alpha_{24}) + R(0, \sigma_{25})$

NOTE: Booster, sustainer, and vernier may be considered as Booster Stages 1, 2, and 3.

Table 1. Selection Process for Parameter Dispersions, Contd

dα	PARAMETER	SELECTION PROCESS
dα_{27}	Thrust	**CENTAUR PROPULSION** $LO2A = NLO2A - d\alpha_{11} - d\alpha_{16} - DLO2R$ $\left\{\begin{array}{l} DLO2R = d\alpha_{14_8} \text{ if FLAG} \neq 1 \\ \text{otherwise,} \\ DLO2R = 0 \end{array}\right.$ $LH2A = NLH2A - d\alpha_{10} - d\alpha_{15} - DLH2R$ $\left\{\begin{array}{l} DLH2R = d\alpha_{14_8} \text{ if FLAG} = 1 \\ \text{otherwise,} \\ DLH2R = 0 \end{array}\right.$ Then, $MR = LO2A/LH2A$ $THSTMR = TCEN\ (MR)$ $ISPMR = ICEN\ (MR)$ (See Figures 1 and 2) $DTE1 = R\ (0,\ \sigma_{27})$ $DTE2 = R\ (0,\ \sigma_{27})$ $DIE1 = R\ (0,\ \sigma_{28})$ $DIE2 = R\ (0,\ \sigma_{28})$ $\dot{\omega}_1 = (THSTMR + DTE1)/(ISPMR + DIE1)$ $\dot{\omega}_2 = (THSTMR + DTE2)/(ISPMR + DIE2)$ Then, $d\alpha_{27} = DTE1 + DTE2 + 2\ (THSTMR - THSTN)$

Table 1. Selection Process for Parameter Dispersions, Contd

$d\alpha$	PARAMETER	SELECTION PROCESS
$d\alpha_{28}$	Specific Impulse (I_{sp})	$d\alpha_{28} = (d\alpha_{27} + 2 \times THSTN)/(\dot{\omega}_1 + \dot{\omega}_2) - ISPN$
$d\alpha_{29}$	Thrust (Burn 2)	
$d\alpha_{30}$	Isp (Burn 2)	Not presently used. Same technique as above would apply.
$d\alpha_{31}$	Thrust (Burn 3)	
$d\alpha_{32}$	I_{sp} (Burn 3)	
$d\alpha_{33}$	Attitude Control (Coast 1)	$d\alpha_{33} = R(0, \sigma_{33})$
$d\alpha_{34}$	Attitude Control (Coast 2)	$d\alpha_{34} = R(0, \sigma_{34})$
$d\alpha_{35}$	Atmosphere	$d\alpha_{35} = R(0, \sigma_{35})$ (see Table 2)
$d\alpha_{36}$	Launch Azimuth	
	Null Voltage	$d\alpha_{36_1} = R(0, \sigma_{36_1})$
	Roll Gyro Torquing Rate	$d\alpha_{36_2} = R(0, \sigma_{36_2})$
	Time Uncertainties	$d\alpha_{36_3} = R(0, \sigma_{36_3})$
	Allowed Tolerance	$d\alpha_{36_4} = R(0, \sigma_{36_4})$
		Then, $$d\alpha_{36} = \sum_{i=1}^{4} d\alpha_{36_i}$$
$d\alpha_{37}$	Pitch Program	
	Voltage-Time Integral	$d\alpha_{37_1} = R(0, \sigma_{37_1})$
	Gyro Torquing Rate-Voltage-Time Avg.	$d\alpha_{37_2} = R(0, \sigma_{37_2})$

Table 1. Selection Process for Parameter Dispersions, Contd

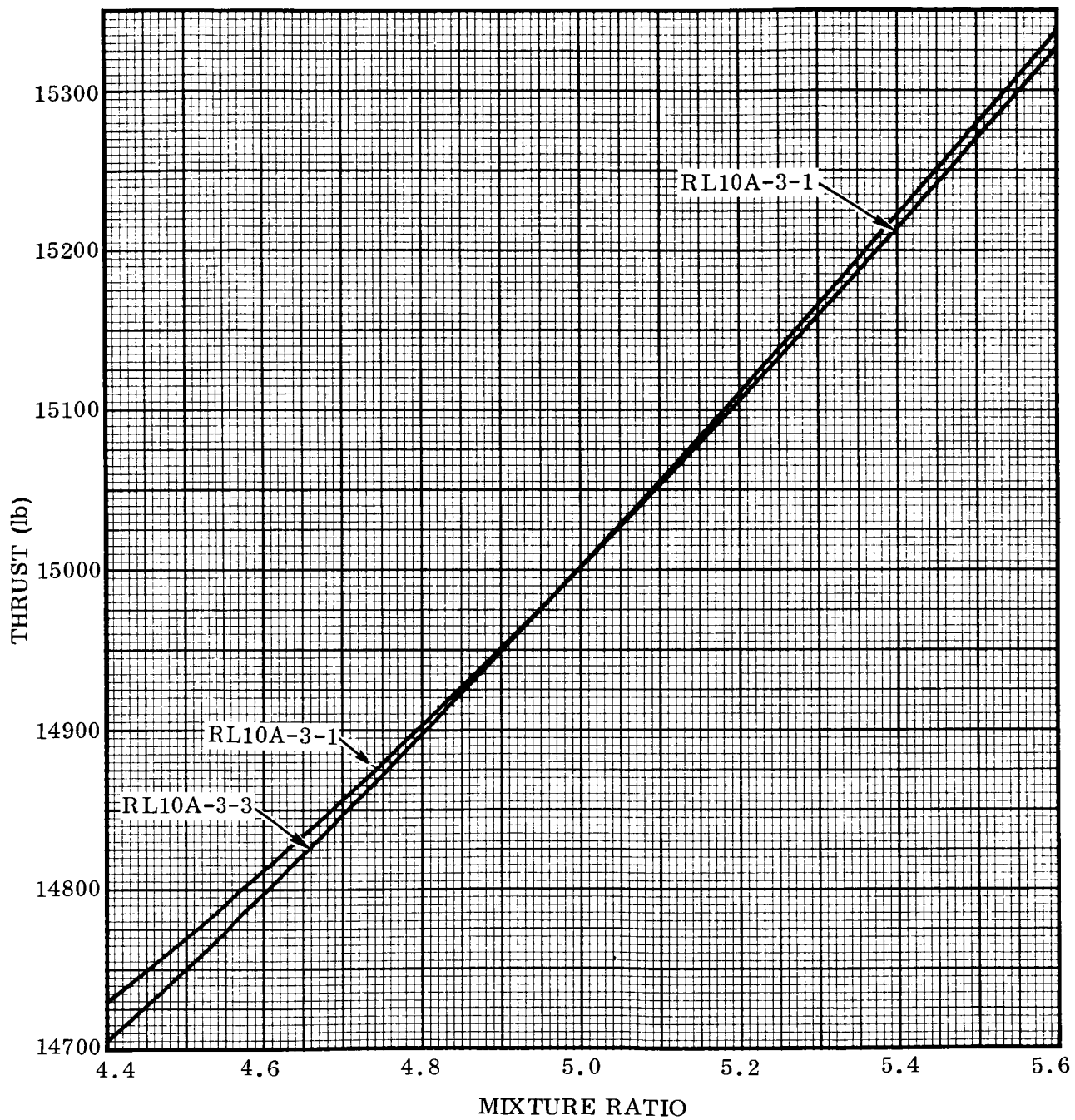| dα	PARAMETER	SELECTION PROCESS
	Inverter Voltage	$d\alpha_{37_3} = R(0, \sigma_{37_3})$
	Inverter Frequency	$d\alpha_{37_4} = R(0, \sigma_{37_4})$
		Then, $$d\alpha_{37} = \sum_{i=1}^{4} d\alpha_{37_i}$$
dα_{38}	Drag Force	$d\alpha_{38} = R(0, \sigma_{38})$ (Through vehicle reference area)
dα_{39}	Wind Profile*	$d\alpha_{39} = R(0, \sigma_{39})$ (see Table 3)
		* Particular wind profile used should be related to a pitch-program-associated period and not to a particular month.

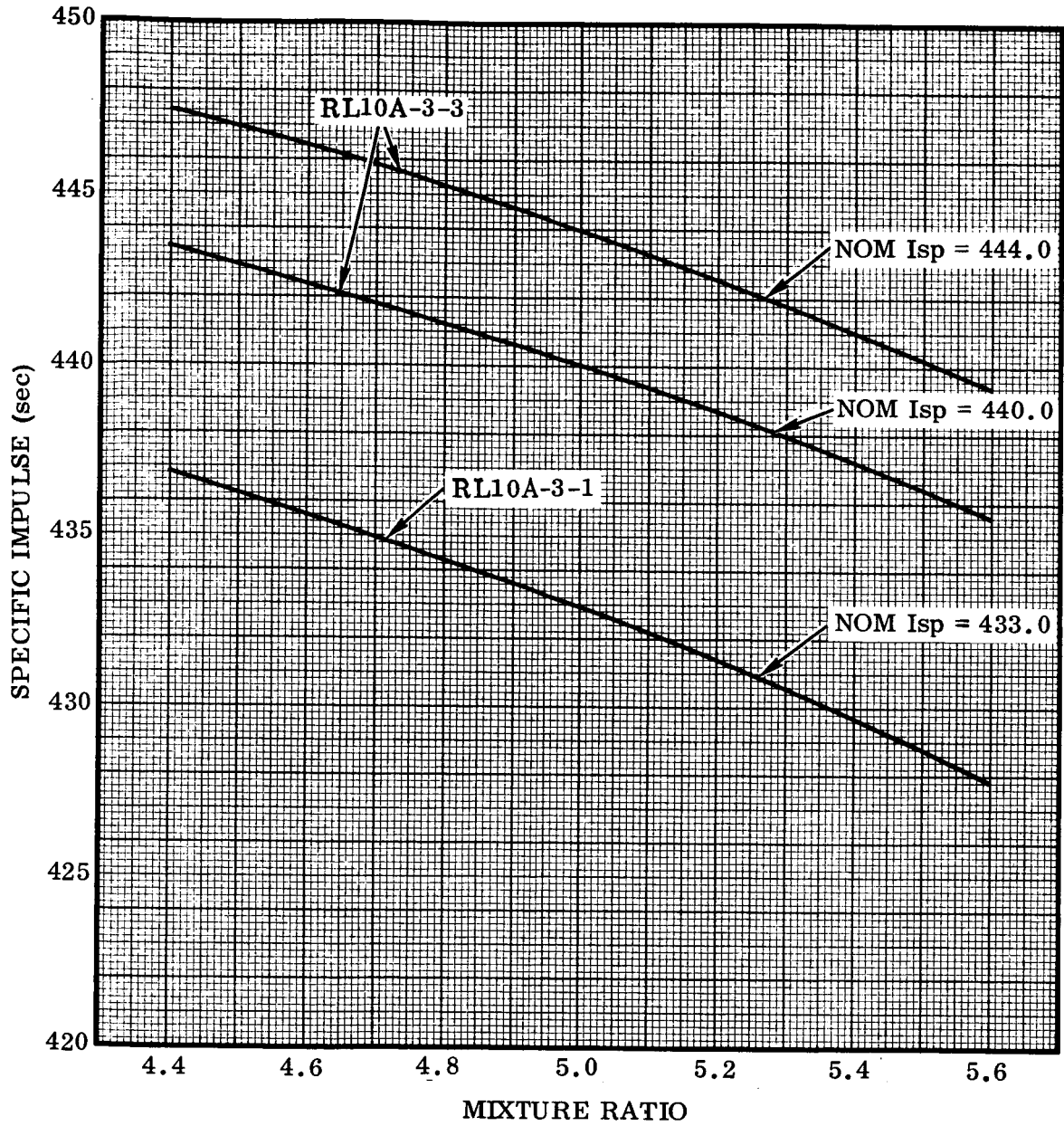Figure 1. Centaur Engine Thrust vs. Mixture Ratio

Figure 2. Centaur Engine Specific Impulse vs. Mixture Ratio

Table 2. Pressure, Density, and Temperature Variations*

ALTITUDE (ft)	INCREASED DENSITY			DECREASED DENSITY			PROBABILITY
	DENSITY	PRESSURE	TEMP	DENSITY	PRESSURE	TEMP	
0	1.080	1.023	0.947	0.960	0.987	1.028	
25,000	1.060	1.017	0.960	0.930	0.978	1.052	
60,000	1.085	1.024	0.944	0.930	0.978	1.052	3σ
300,000	1.525	1.134	0.744	0.660	0.882	1.337	
500,000	2.045	1.239	0.606	0.516	0.819	1.589	
650,000	2.485	1.314	0.528	0.440	0.781	1.776	
0	1.053	1.015	0.964	0.973	0.991	1.019	
25,000	1.040	1.011	0.972	0.953	0.985	1.034	
60,000	1.056	1.016	0.962	0.953	0.985	1.034	2σ
300,000	1.350	1.094	0.810	0.773	0.925	1.197	
500,000	1.696	1.171	0.690	0.677	0.889	1.313	
650,000	1.990	1.229	0.617	0.626	0.869	1.386	
0	1.026	1.007	0.981	0.986	0.995	1.009	
25,000	1.020	1.005	0.986	0.976	0.992	1.016	
60,000	1.028	1.008	0.980	0.976	0.992	1.016	1σ
300,000	1.175	1.049	0.893	0.886	0.964	1.087	
500,000	1.348	1.093	0.811	0.838	0.948	1.131	
650,000	1.495	1.128	0.754	0.813	0.939	1.155	

*Multipliers on standard atmosphere (NASA–Patrick + ARDC 1959) used in Reference 1

20

Table 3. Monthly and Period-Related Wind Variations

MONTH	TAIL WIND					CROSS WIND				
	ALT.	AVER.	L. L.	U. L.	S	ALT.	AVER.	L. L.	U. L.	S
May	2,500	-1.61	-41.50	38.29	16.59	2,500	7.48	-35.02	49.99	17.68
	12,500	8.40	-42.17	58.98	21.04	12,500	0.89	-54.39	56.18	22.99
	21,000	24.43	-38.41	87.28	26.14	21,000	1.01	-59.44	61.48	25.15
	30,000	39.97	-37.55	117.48	32.24	30,000	4.91	-80.16	89.98	35.39
	42,000	66.58	-36.79	169.94	42.99	42,000	6.69	-107.94	121.32	47.68
	57,000	26.51	-33.51	86.53	24.97	57,000	-10.55	-61.33	40.22	21.12
Oct	2,500	-2.38	-43.67	38.90	17.17	2,500	-6.03	-44.99	32.93	16.21
	12,500	14.45	-41.13	70.03	23.12	12,500	-2.53	-35.29	30.23	13.63
	21,000	27.78	-41.87	97.43	28.97	21,000	-2.81	-45.19	39.56	17.63
	30,000	44.80	-62.04	151.64	44.44	30,000	-2.49	-84.00	79.03	33.91
	42,000	64.24	-70.97	199.45	56.25	42,000	-9.84	-105.76	86.08	39.90
	57,000	14.43	-47.78	76.64	25.89	57,000	-3.27	-30.12	23.58	11.17
May & Oct	2,500	-1.99	-38.19	34.20	16.74	2,500	0.72	-38.49	39.94	18.14
	12,500	11.43	-36.40	59.25	22.12	12,500	-0.82	-41.49	39.86	18.81
	21,000	26.11	-33.14	85.36	27.40	21,000	-0.90	-47.62	45.82	21.61
	30,000	42.39	-40.98	125.75	38.56	30,000	1.21	-73.49	75.91	34.55
	42,000	65.41	-41.90	172.72	49.63	42,000	-1.57	-97.50	94.35	44.37
	57,000	20.47	-35.58	76.53	25.93	57,000	-6.91	-43.98	30.16	17.14
June	2,500	4.07	-39.81	47.95	18.25	2,500	11.27	-25.56	48.10	15.32
	12,500	11.13	-27.81	50.07	16.20	12,500	2.93	-30.25	36.12	13.81
	21,000	13.88	-23.79	51.55	15.67	21,000	-0.38	-31.04	30.28	12.75
	30,000	21.28	-37.74	80.30	24.55	30,000	-2.05	-52.49	48.39	20.98
	42,000	31.47	-55.80	118.75	36.30	42,000	-13.84	-89.88	62.19	31.63
	57,000	-3.69	-41.04	33.66	15.54	57,000	-9.41	-38.69	19.88	12.18
July	2,500	2.01	-26.87	30.88	12.11	2,500	9.08	-13.51	31.68	9.48
	12,500	2.52	-21.37	26.41	10.02	12,500	2.97	-14.85	20.79	7.47
	21,000	-1.02	-27.81	25.78	11.23	21,000	-0.55	-31.23	30.13	12.86
	30,000	-5.67	-44.35	33.01	16.22	30,000	-5.37	-48.35	37.61	18.02
	42,000	-15.91	-83.22	51.40	28.22	42,000	-17.37	-91.56	56.83	31.11
	57,000	-21.20	-56.55	14.15	14.82	57,000	-4.98	-30.12	20.16	10.54

Table 3. Monthly and Period-Related Wind Variations, Contd

MONTH	TAIL WIND					CROSS WIND				
	ALT.	AVER.	L.L.	U.L.	S	ALT.	AVER.	L.L.	U.L.	S
Aug	2,500	1.53	-29.49	32.55	12.90	2,500	8.94	-13.09	30.97	9.16
	12,500	1.32	-35.24	37.89	15.21	12,500	7.48	-25.20	40.17	13.60
	21,000	-0.86	-32.11	30.38	13.00	21,000	2.82	-34.26	39.90	15.42
	30,000	-5.96	-43.68	31.75	15.69	30,000	-0.92	-45.68	43.84	18.62
	42,000	-8.95	-71.80	53.89	26.14	42,000	-7.96	-72.84	56.92	26.99
	57,000	-20.51	-41.87	0.85	8.89	57,000	-3.38	-32.59	25.82	12.15
Sept	2,500	-5.38	-48.58	37.82	18.11	2,500	-0.83	-62.52	60.86	25.87
	12,500	-0.88	-47.45	45.69	19.53	12,500	0.18	-31.02	31.38	13.08
	21,000	0.21	-47.96	48.37	20.20	21,000	-3.52	-44.72	37.67	17.27
	30,000	4.05	-58.92	67.01	26.40	30,000	-7.95	-60.23	44.33	21.92
	42,000	7.16	-85.92	100.24	39.03	42,000	-17.87	-93.06	57.31	31.52
	57,000	-11.92	-59.83	35.99	20.09	57,000	-5.27	-41.67	31.12	15.26
June	2,500	0.52	-33.67	34.71	15.81	2,500	7.07	-29.54	43.67	16.93
July	12,500	3.48	-31.27	38.23	16.07	12,500	3.36	-23.38	30.10	12.37
Aug	21,000	2.99	-32.58	38.57	16.45	21,000	-0.43	-32.20	31.33	14.69
&	30,000	3.35	-47.96	54.66	23.73	30,000	-4.11	-47.12	38.89	19.89
Sept	42,000	3.31	-77.19	83.81	37.23	42,000	-14.32	-79.74	51.10	30.26
	57,000	-14.37	-50.69	21.95	16.80	57,000	-5.75	-33.18	21.68	12.69
Jan	2,500	3.44	-53.07	59.96	23.70	2,500	12,20	-65.84	90.24	32.72
	12,500	50.24	-15.99	116.47	27.77	12,500	10.41	-64.86	85.68	31.56
	21,000	80.76	-0.83	162.35	34.21	21,000	15.68	-52.93	84.29	28.77
	30,000	124.09	-16.29	264.47	58.86	30,000	11.56	-102.75	125.86	47.93
	42,000	149.64	35.88	263.41	47.70	42,000	19.59	-95.77	134.95	48.37
	57,000	101.34	-21.68	224.35	51.58	57,000	11.16	-66.60	88.93	32.61
Feb	2,500	11.09	-48.67	70.85	24.86	2,500	6.89	-52.87	66.65	24.86
	12,500	49.01	-21.13	119.15	29.17	12,500	8.66	-53.51	70.83	25.86
	21,000	78.90	8.81	148.99	29.16	21,000	15.53	-47.04	78.10	26.03
	30,000	123.67	-3.23	250.57	52.79	30,000	28.08	-76.59	132.75	43.54
	42,000	159.03	23.56	294.49	56.34	42,000	26.22	-83.49	135.92	45.63
	57,000	89.23	16.39	162.07	30.30	57,000	12.21	-48.95	73.37	25.44
Apr	2,500	-0.97	-47.21	45.25	19.07	2,500	6.09	-50.26	62.43	23.25
	12,500	33.57	-43.37	110.50	31.74	12,500	-1.01	-53.82	51.79	21.78
	21,000	52.00	-36.82	140.83	36.64	21,000	3.17	-54.00	60.35	23.59

Table 3. Monthly and Period-Related Wind Variations, Contd

MONTH	TAIL WIND					CROSS WIND				
	ALT.	AVER.	L.L	U.L.	S	ALT.	AVER.	L.L.	U.L.	S
	30,000	99.47	-47.50	246.44	60.63	30,000	2.54	-75.34	80.42	32.13
	42,000	132.21	-21.83	286.25	63.55	42,000	-2.81	-115.68	110.05	46.56
	57,000	69.02	-58.10	196.14	52.44	57,000	-4.62	-55.56	46.32	21.01
Mar	2,500	10.88	-41.10	62.86	21.44	2,500	8.74	-53.95	71.42	25.86
	12,500	53.66	-18.76	126.07	29.87	12,500	5.55	-73.62	84.71	32.66
	21,000	88.13	19.06	157.19	28.49	21,000	6.03	-72.27	84.34	32.30
	30,000	123.83	34.72	212.94	36.76	30,000	16.00	-86.48	118.49	42.28
	42,000	160.77	57.11	264.43	42.76	42,000	17.43	-99.64	134.50	48.30
	57,000	100.01	-21.33	221.36	50.06	57,000	10.52	-53.79	74.84	26.53
Dec	2,500	-4.26	-50.87	42.35	19.39	2,500	-0.44	-51.57	50.69	21.27
	12,500	28.39	-19.44	76.21	19.89	12,500	6.44	-34.98	47.86	17.23
	21,000	56.89	-19.48	133.27	31.77	21,000	9.32	-39.61	58.25	20.35
	30,000	90.82	-10.23	191.87	42.03	30,000	11.17	-72.98	95.33	35.01
	42,000	118.39	14.85	221.92	43.07	42,000	11.81	-135.60	159.23	61.32
	57,000	80.91	3.14	158.67	32.35	57,000	20.24	-50.98	91.45	29.62
Nov	2,500	-0.93	-38.59	36.72	15.79	2,500	-4.69	-43.70	34.31	16.35
	12,500	16.88	-27.39	61.16	18.56	12,500	-2.47	-47.61	42.68	18.93
	21,000	33.14	-33.10	99.39	27.78	21,000	-2.49	-56.96	51.98	22.84
	30,000	52.93	-37.31	143.16	37.83	30,000	-3.47	-83.79	76.86	33.68
	42,000	76.99	-20.75	174.73	40.98	42,000	-10.97	-135.76	113.83	52.33
	57,000	37.47	-17.00	91.95	22.84	57,000	-2.41	-48.89	44.07	19.49
Nov	2,500	3.16	-43.23	49.55	21.46	2,500	4.76	-49.05	58.57	24.89
Dec	12,500	38.51	-25.15	102.17	29.45	12,500	4.61	-50.37	59.61	25.43
Jan	21,000	64.82	-14.29	143.92	36.59	21,000	7.90	-49.14	64.94	26.38
Feb	30,000	102.20	-16.66	221.06	54.98	30,000	10.92	-76.13	97.97	40.27
Mar	42,000	132.46	9.04	255.87	57.08	42,000	10.18	-101.57	121.92	51.69
Apr	57,000	78.51	-22.33	179.34	46.64	57,000	7.87	-51.06	66.79	27.26

NOTE: Confidence = 90%   L.L. = Lower Limit

Probability = 99%   U.L. = Upper Limit

Tail Wind Positive When From West   S   = Standard Deviation

Cross Wind Positive When From South

SECTION 5

RESULTS

The model outlined has been used to evaluate FPR requirements for a typical direct ascent Atlas/Centaur/Surveyor mission. The performance partials derived for this study (Table 4) were computed at three intervals during a typical window to observe changes in FPR within that time (Figure 3). Injection flight path angle variation was from -4 to 6 degrees. A PU system bias setting of 60 pounds with an uncertainty of ±90 pounds was used as a reference. A total of 10,000 iterations on performance were computed for each FPR value. Individual parameter variations were obtained from Reference 2.

Figure 4 presents the parametric results of the study showing the influence of PU system accuracy and bias on net payload capability. The values on Figure 4 will be reduced essentially by the function across the window (Figure 3). Figure 5 gives the equivalent enveloping function for the data. The FPR requirements for a given system uncertainty at an optimum bias setting are presented in Figure 6. This data shows that, for a PU System uncertainty of ±25 pounds, the FPR is 145 pounds with a payload capability gain of 86 pounds.

Figures 7, 8 and 9 present frequency and probability functions as obtained directly from the computer program. These results, which correspond to the ±25 pound PU system uncertainty and optimum bias (9 pounds), exhibit a negatively skewed FPR because of biased Centaur tanking procedures.

In conclusion, the analysis described herein has provided increased confidence in establishment of FPR values for Atlas/Centaur in addition to realizing a significant potential payload capability gain.

Table 4. FPR Partial Derivatives for Parameters Over Range
of Variation - Atlas/Centaur

α_i	$\begin{array}{c}\text{max}\\\text{min}\end{array} d\alpha_i$	$\partial f/\partial \alpha_i$ (lb/unit)*		
		$\gamma = -3.9°$	$\gamma = 1.6°$	$\gamma = 5.6°$
1	±30 lb	+ 0.0539	+ 0.0328	+ 0.0304
		+ 0.0440	+ 0.0741	+ 0.1059
2	±69 lb	+ 0.0986	+ 0.0874	+ 0.0672
		+ 0.0913	+ 0.0932	+ 0.1095
3	±59 lb	+ 0.9101	+ 0.9196	+ 0.9393
		+ 0.9288	+ 0.9385	+ 0.9849
4	±75 lb	+ 0.0807	+ 0.0810	+ 0.0537
		+ 0.0740	+ 0.0681	+ 0.0744
5	±48 lb	+ 0.0768	+ 0.0548	+ 0.0407
		+ 0.0570	+ 0.0609	+ 0.0832
6	±847 lb	− 0.0144	− 0.0181	− 0.0188
		− 0.0282	− 0.0288	− 0.0275
7	±0.55 lb/cu.ft.	− 9.2854	− 16.1405	− 19.6182
		− 33.9791	− 36.1342	− 39.2711
8	±1269 lb	− 0.0060	− 0.0087	− 0.0094
		− 0.0110	− 0.0123	− 0.0134
9	±0.4635 lb/cu.ft.	− 37.3752	− 36.7873	− 37.7612
		− 48.9948	− 46.9105	− 41.7907
10 ⎱ 11 ⎰	+500 lb −409 lb	− 0.0878 − 0.0956	− 0.0709 − 0.0755	− 0.0389 − 0.0538
12	±87 lb	+ 0.0776	+ 0.0690	+ 0.0510
		+ 0.0653	+ 0.0703	+ 0.0728
13	⎰+276 lb ⎱−259 lb	+ 0.1073 + 0.1076	+ 0.1066 + 0.1099	+ 0.1034 + 0.1095
14 ⎱ 15 ⎰	±100 lb	+ 1.0000 + 1.0000	+ 1.0000 + 1.0000	+ 1.0000 + 1.0000

*Partial derivative of FPR with respect to α_i. Values derived using closed-loop guidance simulation. Parameters for which no values appear were not considered significant or applicable in the present study.

Table 4. FPR Partial Derivatives for Parameters Over Range
of Variation - Atlas/Centaur, Contd

α_i	$\begin{array}{c}\text{max}\\\text{min}\end{array} d\alpha_i$	$\partial f/\partial \alpha_i$ (lb/unit)*		
		$\gamma = -3.9°$	$\gamma = 1.6°$	$\gamma = 5.6°$
16				
17				
18	±0.023	-115.5217 -397.0870	-113.2174 -353.6087	-175.6957 -312.0435
19	±3000 lb.	- 0.0062 - 0.0065	- 0.0040 - 0.0040	- 0.0026 - 0.0026
20	±2.4 sec	- 18.6318 - 20.0180	- 18.6950 - 18.8711	- 19.3641 - 19.1907
21				
22	±855 lb	+ 0.0124 + 0.0091	+ 0.0092 + 0.0091	+ 0.0050 + 0.0056
23	±2.8 sec	- 14.9448 - 16.1847	- 15.0036 - 15.4210	- 14.8522 - 14.7987
24				
25				
26				
*27	±424 lb	+ 0.0229 + 0.0204	- 0.0114 - 0.0099	- 0.0360 - 0.0452
28	±3.54 sec	- 26.4467 - 26.8088	- 25.9252 - 25.9483	- 24.7464 - 24.6510
29				

*Partial derivative of FPR with respect to α_i. Values derived using closed-loop guidance simulation. Parameters for which no values appear were not considered significant or applicable in the present study.

Table 4. FPR Partial Derivatives for Parameters Over Range
of Variation - Atlas/Centaur, Contd

α_i	max min $d\alpha_i$	$\partial f/\partial \alpha_i$ (lb/unit)*		
		$\gamma = -3.9°$	$\gamma = 1.6°$	$\gamma = 5.6°$
30				
31				
32				
33				
34				
35	±3σ	+ 7.1319 + 8.8700	+ 6.3237 + 7.3709	+ 6.2531 + 7.1063
36	±2 deg	+ 1.4338 - 3.7192	+ 3.6507 - 4.4804	+ 4.4837 - 10.2925
37	±5%	+ 3.8702 - 1.2046	- 5.6079 - 11.2546	- 6.9401 - 12.6088
38	±5%	+ 2.4500 + 2.1067	+ 2.0536 + 2.0455	+ 1.7633 + 2.1701
39	±3σ	- 2.9368 - 0.4899	- 2.8836 - 0.5767	- 1.2529 + 0.0730

*Partial derivative of FPR with respect to α_i. Values derived using closed-loop
guidance simulation. Parameters for which no values appear were not considered
significant or applicable in the present study.

Similar analyses for any booster/Centaur combination can now be quickly handled.
While the major FPR contributers have been simply correlated by the above methods,
further effort along these lines may be required as our knowledge of parameter inter-
action increases.
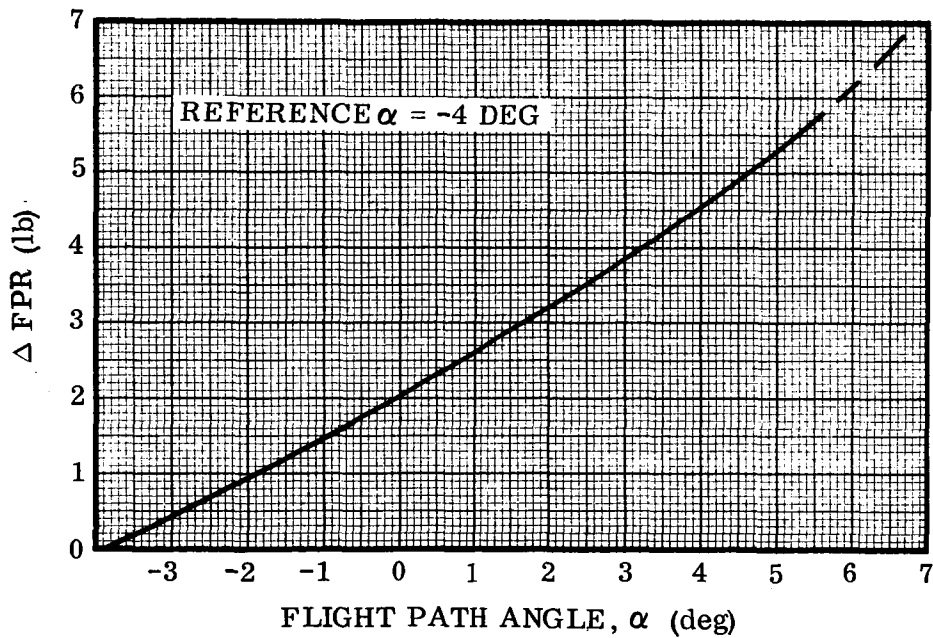
Figure 3. FPR vs. Injection Flight Path Angle

ALL NUMBERS REFERENCED TO A PU
SYSTEM OF 60 ± 90 POUNDS AND AN
FPR OF 180 POUNDS. NOMINAL MIXTURE
RATIO IS 5:1. NET PAYLOAD GAIN
EQUALS THE CHANGE IN FPR PLUS THE
CHANGE IN BIAS REQUIREMENT.
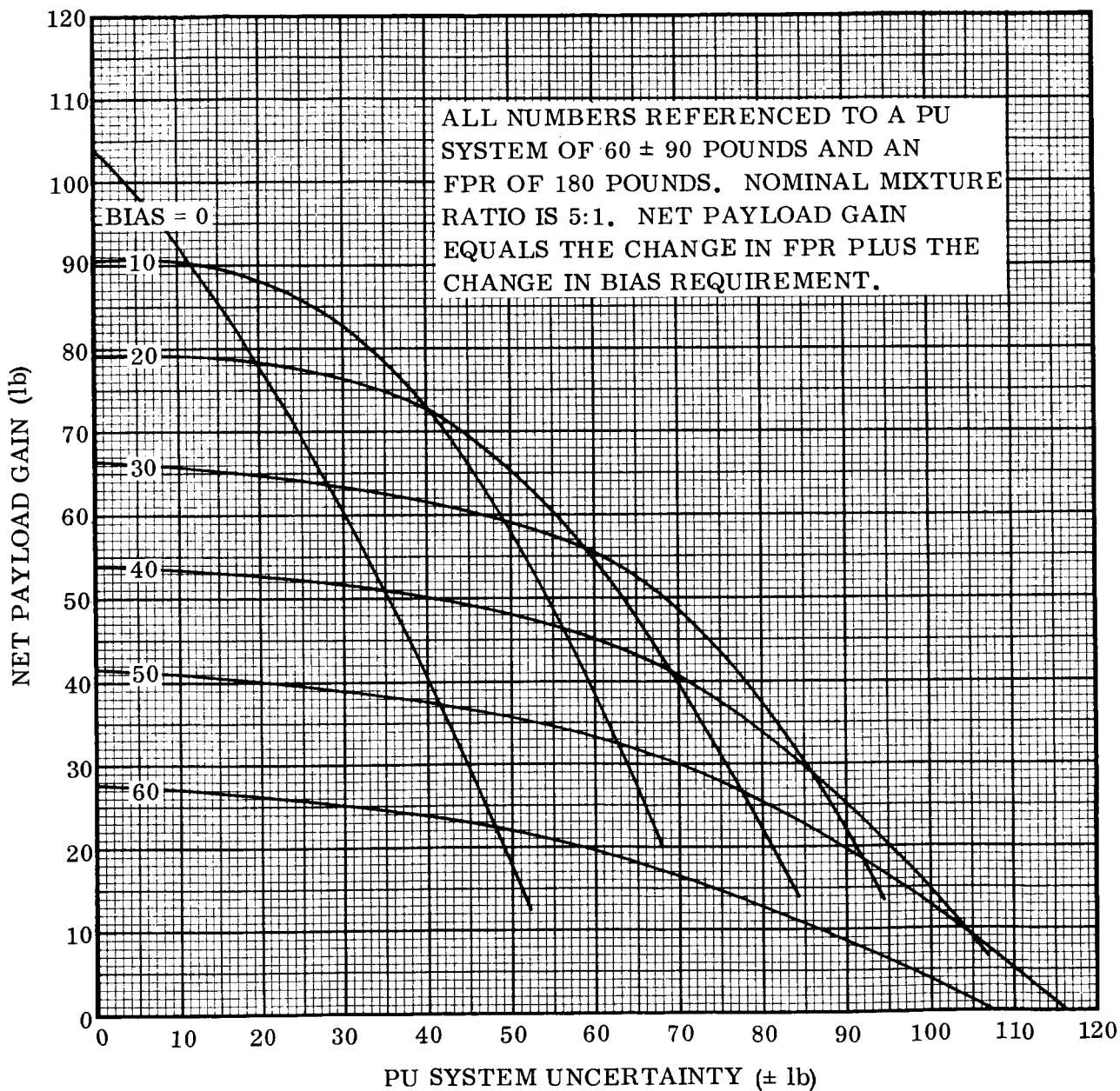
Figure 4. PU System Uncertainty vs. Net Performance Gain

30
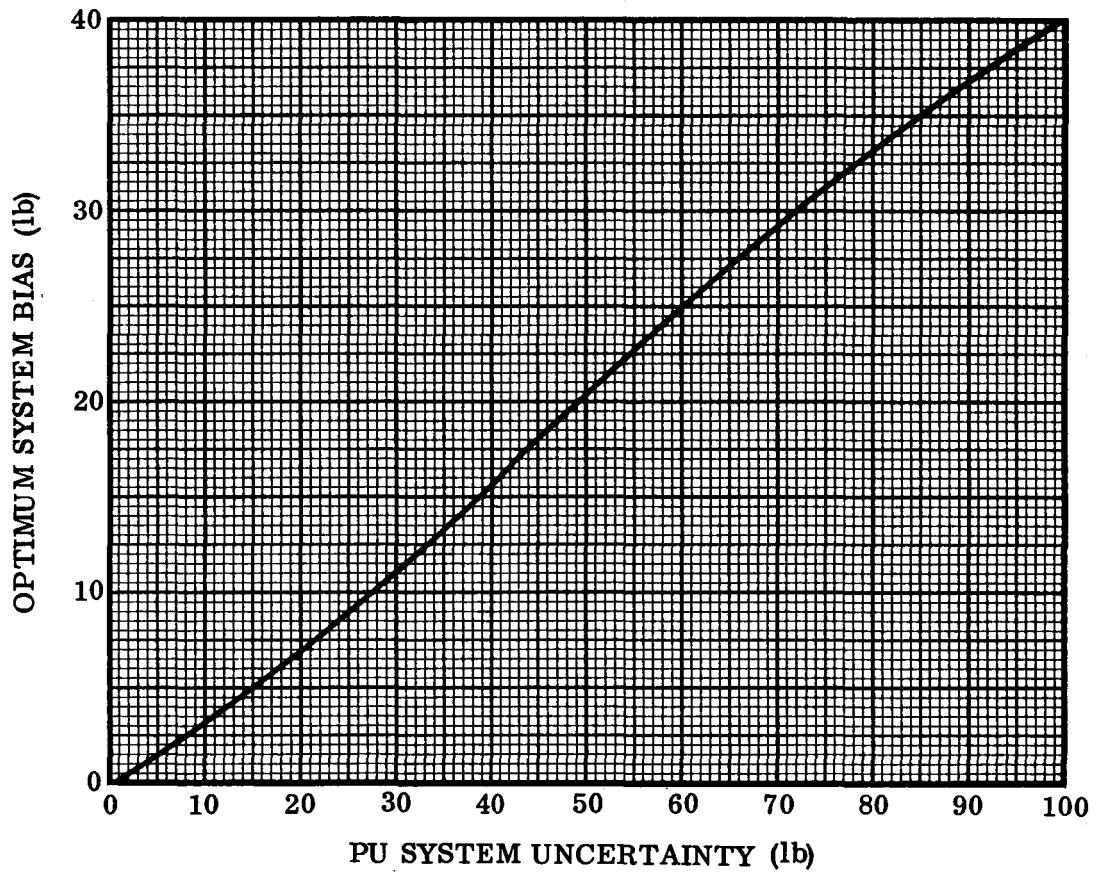
Figure 5. PU System Uncertainty vs. Optimum System Bias
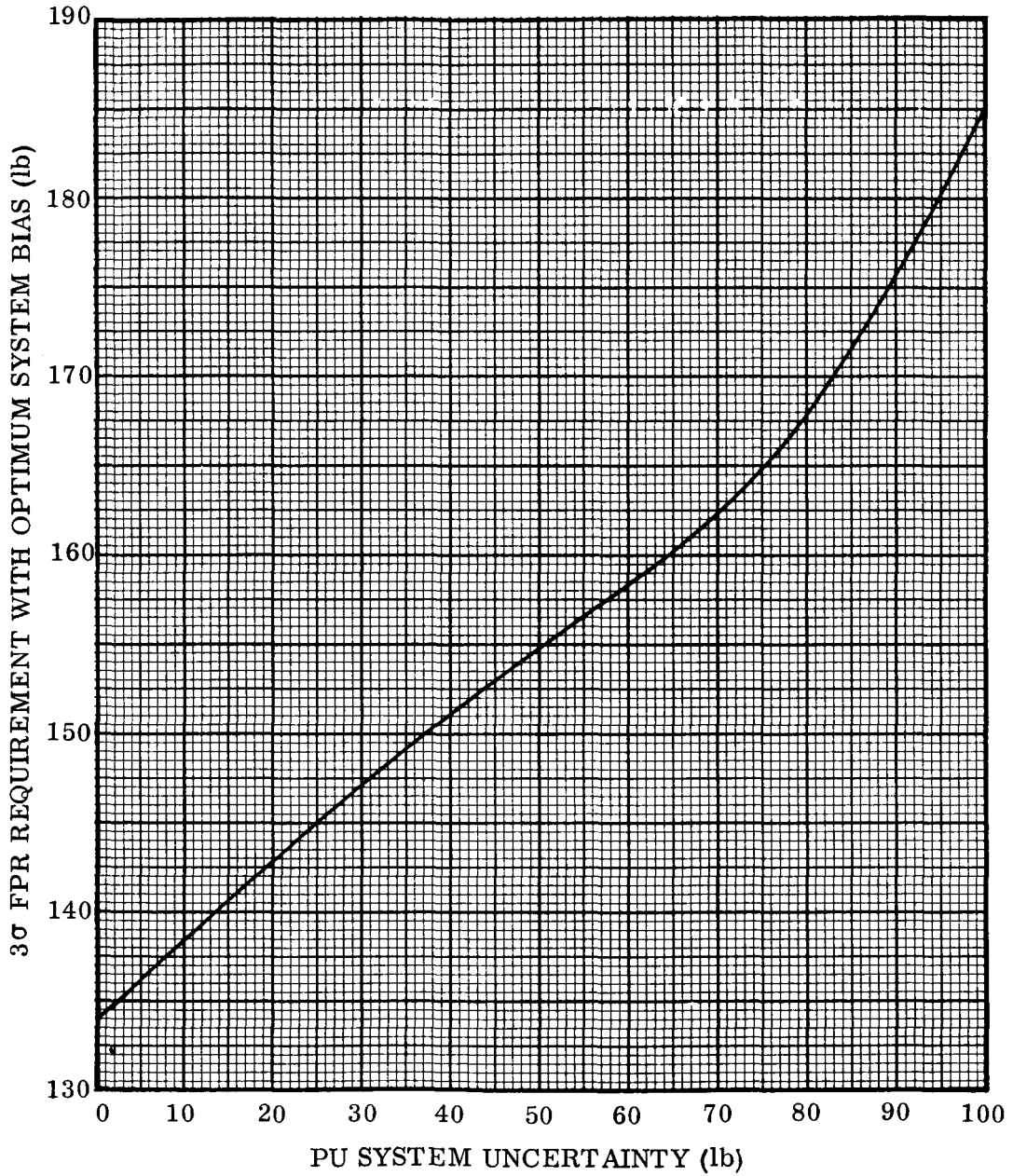
Figure 6. PU System Uncertainty vs. FPR for Optimum System Bias
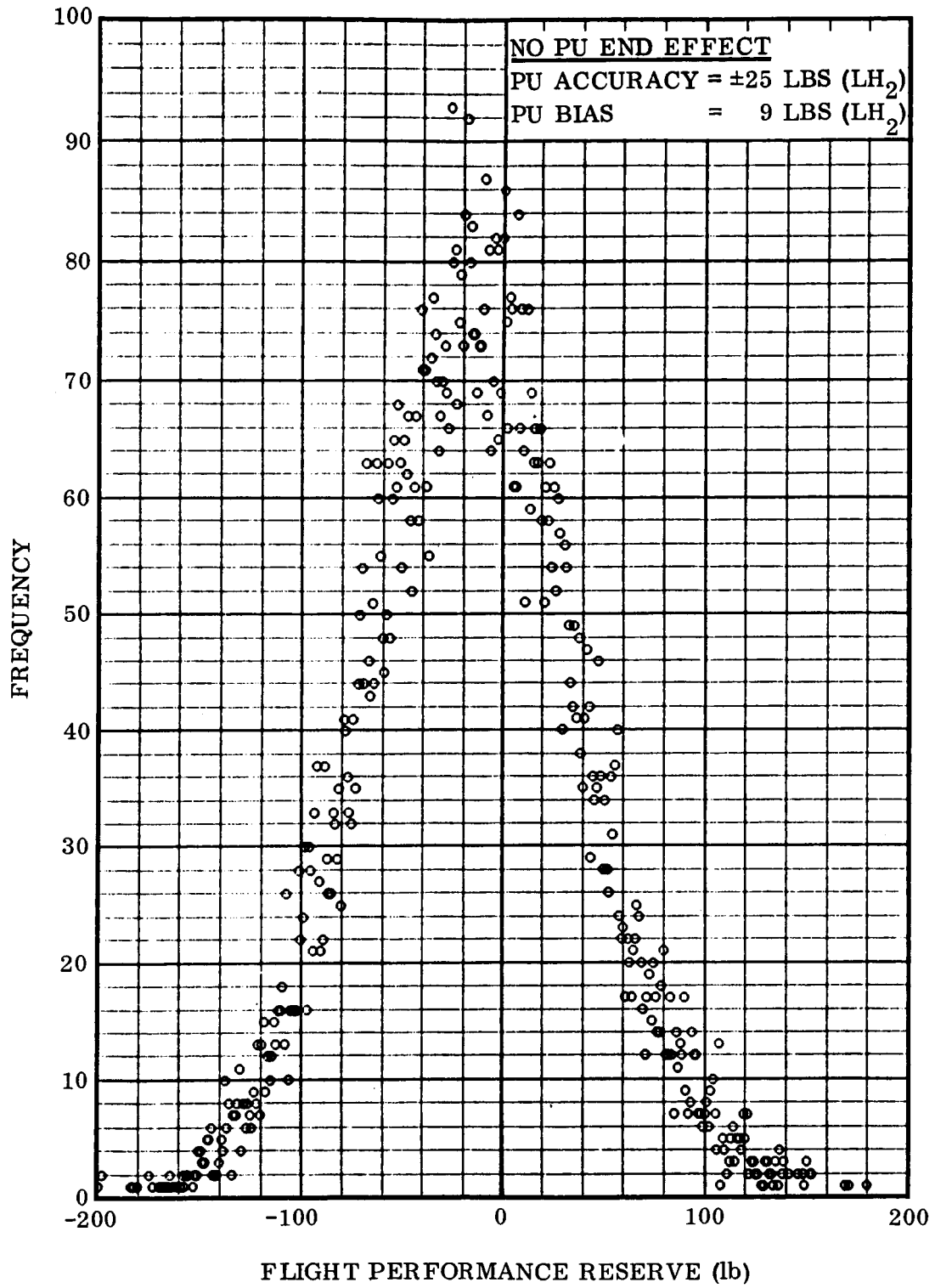
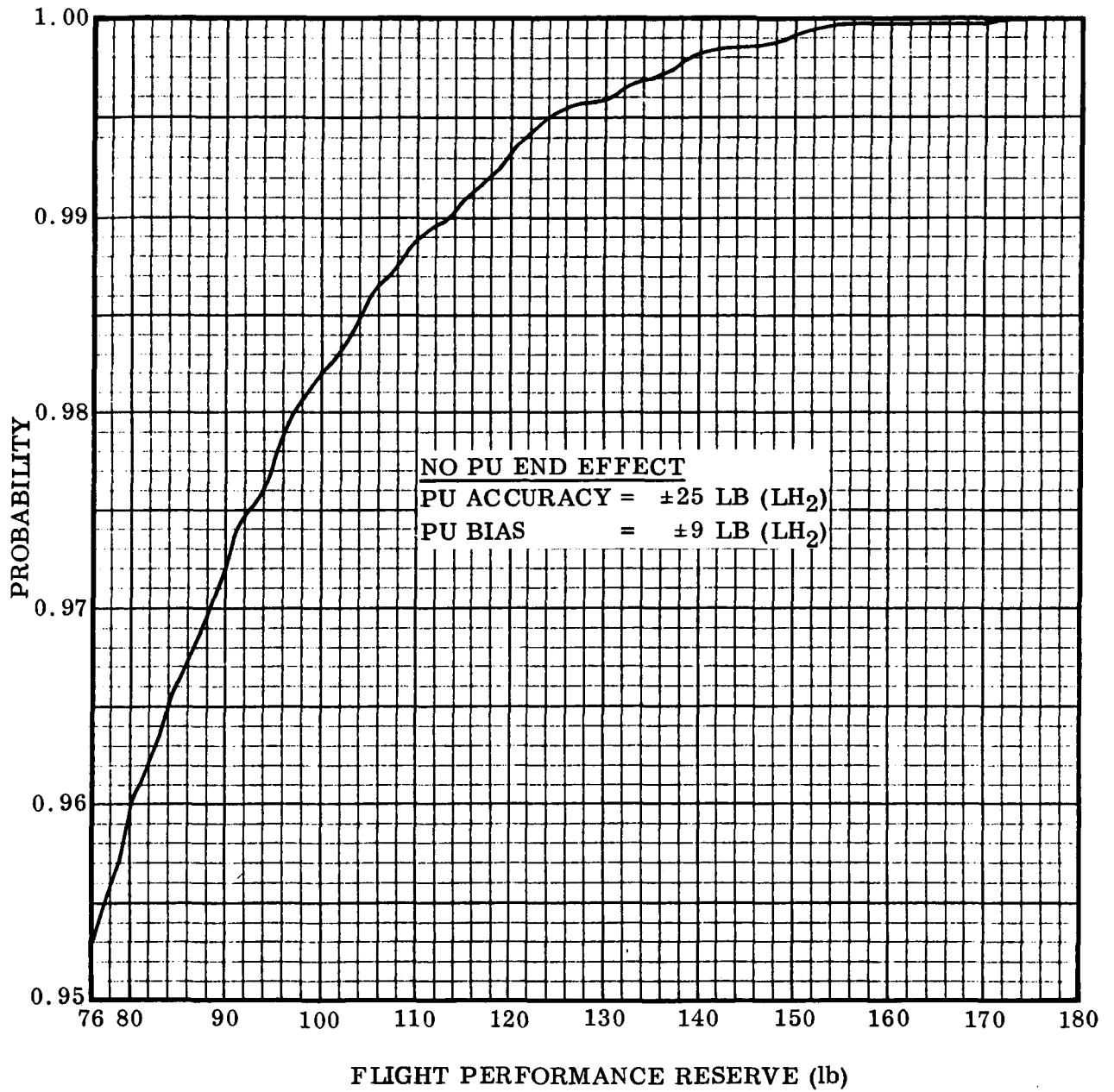Figure 7. FPR Frequency Function
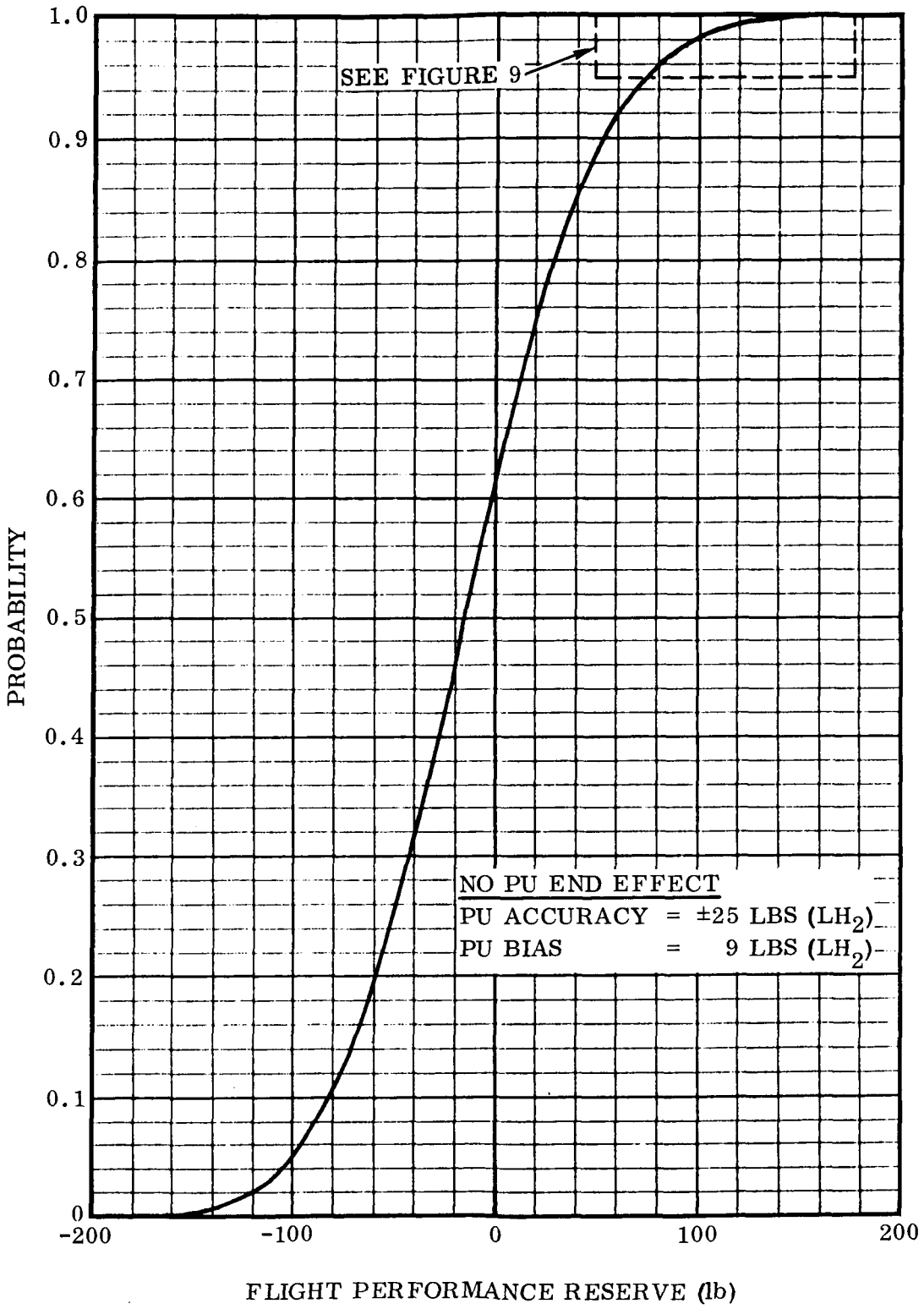
Figure 8. FPR Probability Function

34

NO PU END EFFECT
PU ACCURACY = ±25 LB (LH$_2$)
PU BIAS = ±9 LB (LH$_2$)

PROBABILITY

FLIGHT PERFORMANCE RESERVE (lb)

Figure 9. FPR Probability Function Segment

35/36

SECTION 6

DEFINITIONS

BFDD	Booster Fuel density dispersion
NFTV	Nominal booster fuel tank volume
NBFD	Nominal booster fuel density
BODD	Booster oxidizer density dispersion
NOTV	Nominal booster oxidizer tank volume
NBOD	Nominal booster oxidizer density
CFDD	Centaur Fuel density dispersion
NLH2D	Nominal LH_2 density
NLH2V	Nominal LH_2 volume
MFUV	Mean fuel ullage volume
NLO2D	Nominal LO_2 density
NLO2V	Nominal LO_2 volume
MOUV	Mean oxidizer ullage volume
MGO2TG	Mean GO_2 in tank – ground
SPUB	Sustainer PU bias
CPUB	Centaur PU bias
PUSET	Nominal PU mixture ratio setting
T_B	Polynomial: Δ booster thrust vs. mixture ratio
I_B	Polynomial: Δ booster I_{sp} vs. mixture ratio
T_S	Polynomial: Δ sustainer thrust vs. mixture ratio
I_S	Polynomial: Δ sustainer I_{sp} vs. mixture ratio
T_V	Polynomial: Δ vernier thrust vs. mixture ratio
I_V	Polynomial: Δ vernier I_{sp} vs. mixture ratio
LO2A	LO_2 available for main impulse
NLO2A	Nominal LO_2 available for main impulse
DLO2R	Delta LO_2 residual

37

DEFINITIONS, Contd

DLH2R	Delta LH_2 residuals
MR	Average mixture ratio for entire burn
THSTMR	Nominal thrust at given mixture ratio
TCEN	Polynomial: Thrust vs. mixture ratio
ISPMR	Nominal specific impulse at given mixture ratio
ICEN	Polynomial: I_{sp} vs. mixture ratio
DTE1	Delta thrust, engine 1
DTE2	Delta thrust, engine 2
DIE1	Delta I_{sp}, engine 1
DIE2	Delta I_{sp}, engine 2
THSTN	Nominal thrust at nominal mixture ratio
ISPN	Nominal I_{sp} at nominal mixture ratio
SUBBIAS	Fixed amount of PU bias below LH_2 probe
LBP	Usable LO_2 below probe plus a random dispersion associated with uncovery level
HBP	Usable LH_2 below probe plus a random dispersion associated with uncovery level
VALVLAG	Average time required for the PU system mixture ratio control valve to travel from its position (approximately null) to the maximum or minimum stops
MAXSET	Maximum PU system mixture ratio valve setting
MINSET	Minimum PU system mixture ratio valve setting

SECTION 7

REFERENCES

1. The Combo Flight Program, Report No. GDA63-0967, 15 November 1963.

2. Atlas/Centaur Performance Dispersions, Report No. GD|C-BTD65-057, 23 April 1965.

3. Error Analysis of the Centaur Stage Propellant Utilization Control System, Report No. GD|C-BTD65-141, (Unpublished).

4. Centaur Monthly Configuration, Performance and Weights Status Report, Report No. GDC63-0495-28, 21 September 1965.

APPENDIX

FPR ANALYSIS WITH PU END EFFECT

The preceding analysis makes the assumption that the PU system operates at the null mixture ratio after either LO_2 or LH_2 propellant level falls below the bottom of the PU probes. Late in this study it was ascertained that this assumption was invalid for the existing hardware and circuit logic. The following discussion treats FPR analysis with PU "End Effect" in detail since it is a major contributor to FPR and PU bias.

If the liquid oxygen probe in the Centaur tank is uncovered first, implying a constant sensed LO_2 level, then the system will burn liquid-oxygen rich until depletion. Similarly, if the hydrogen probe is uncovered first, the system, sensing no further LH_2 level change, will burn hydrogen rich until depletion. This mode of operation appears to be out of phase with the requirement for minimum residuals at engine cutoff. Calculations, Figure 10, show the payload capability loss under such operation to be 30 pounds as compared to the no "End Effect" case.

Figures 11, 12 and 13 present frequency and probability distributions as obtained from the program for the case of ±25 pound PU system uncertainty and optimum PU bias (22 pounds) with PU "End Effect." Including the "End Effect" skews the FPR in the positive direction because of the non-symmetric PU residual distribution.

Modifications to the FPR model which have been added to permit analysis with PU "End Effect" are presented below.

First, let R_1 be a random variate from a PU system uncertainty distribution. If

$$R_1 \geq - \text{(CPUB-SUBBIAS)}$$

then the LO_2 probe is uncovered first. Otherwise, the LH_2 probe is uncovered first.

Consider the situation at LO_2 probe uncovery. There are LBP pounds of liquid oxygen at this time. Also, there are
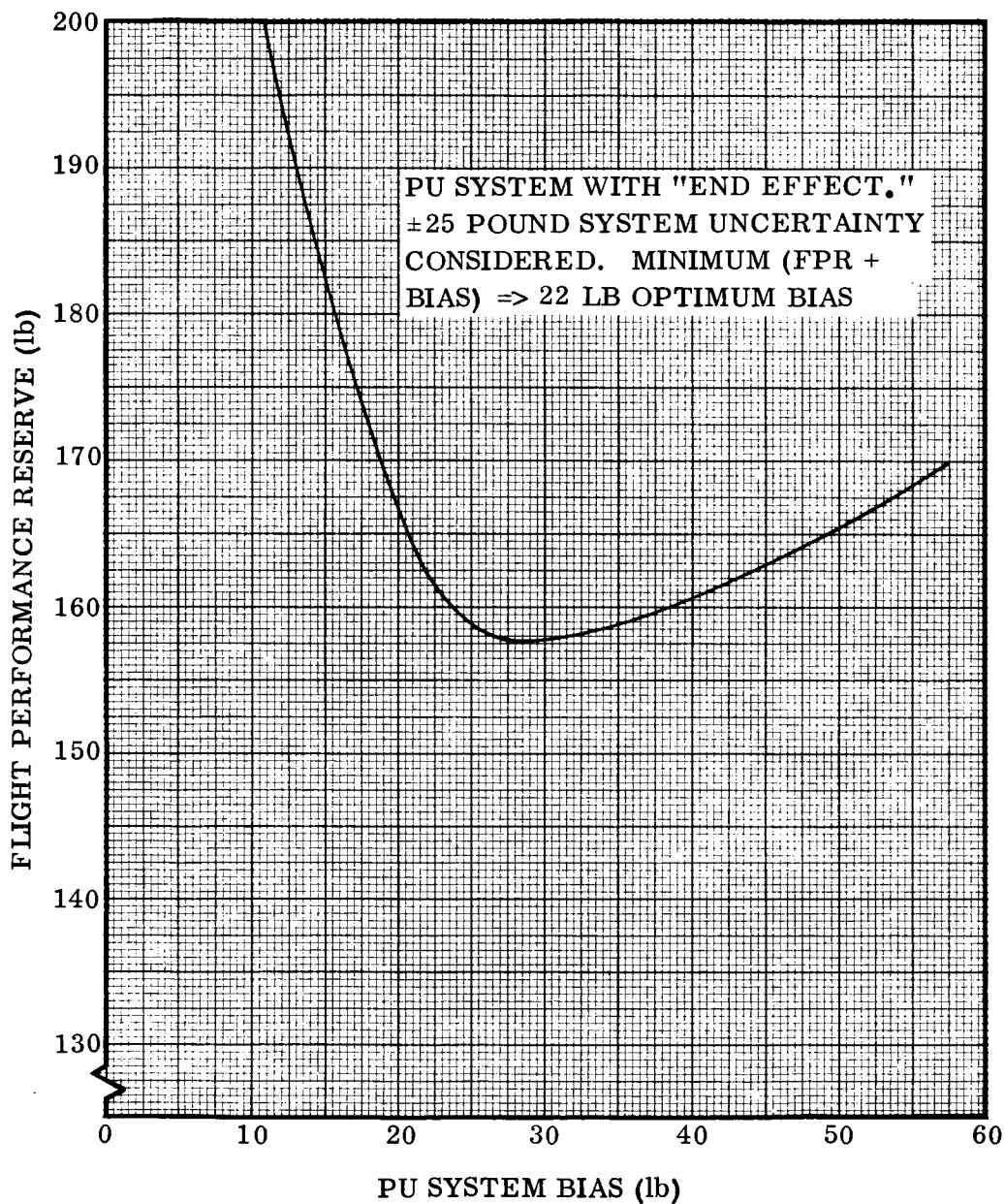
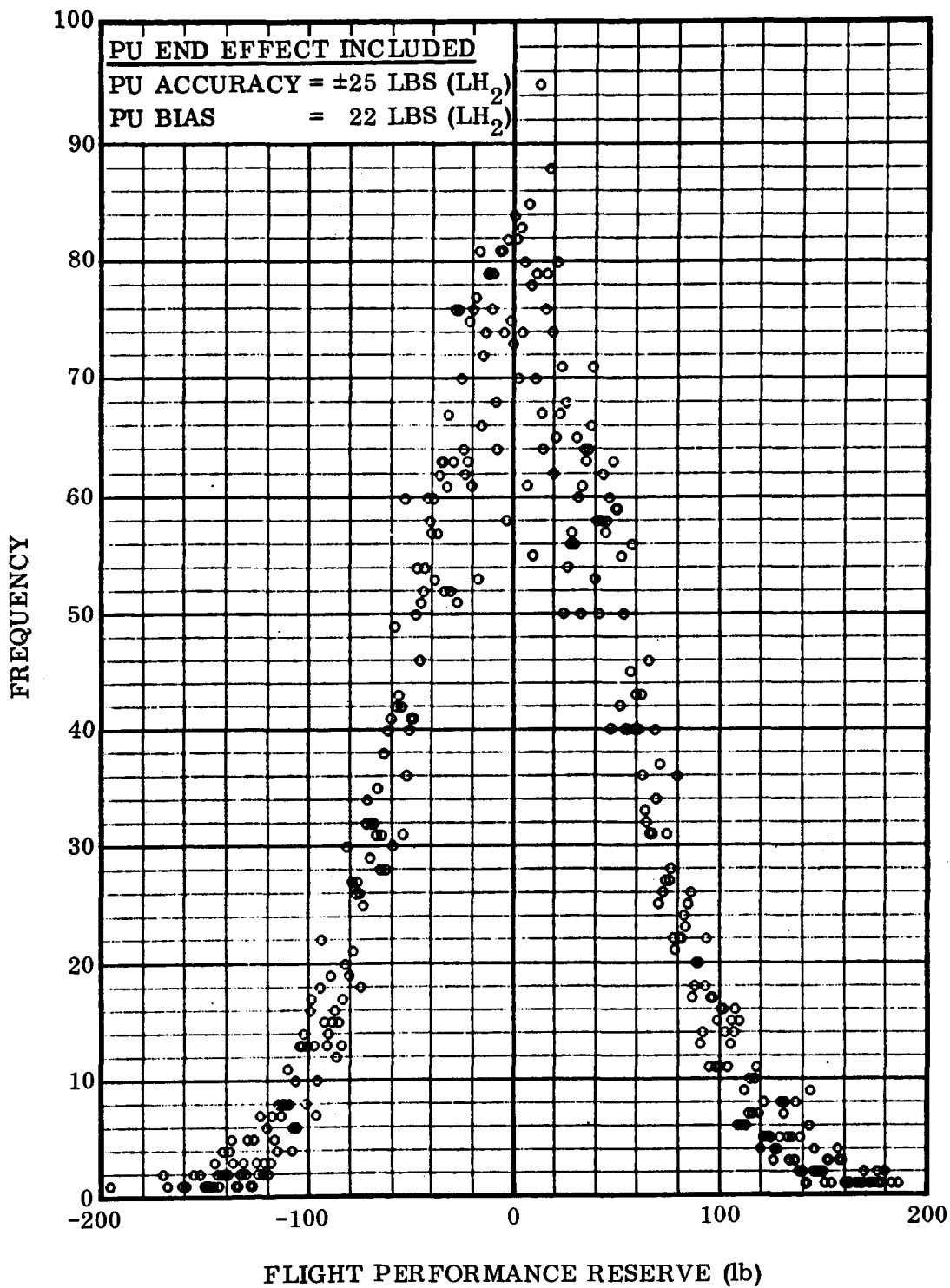Figure 10. PU System Bias vs. FPR for ±25 Pound System Uncertainty with End Effect

42

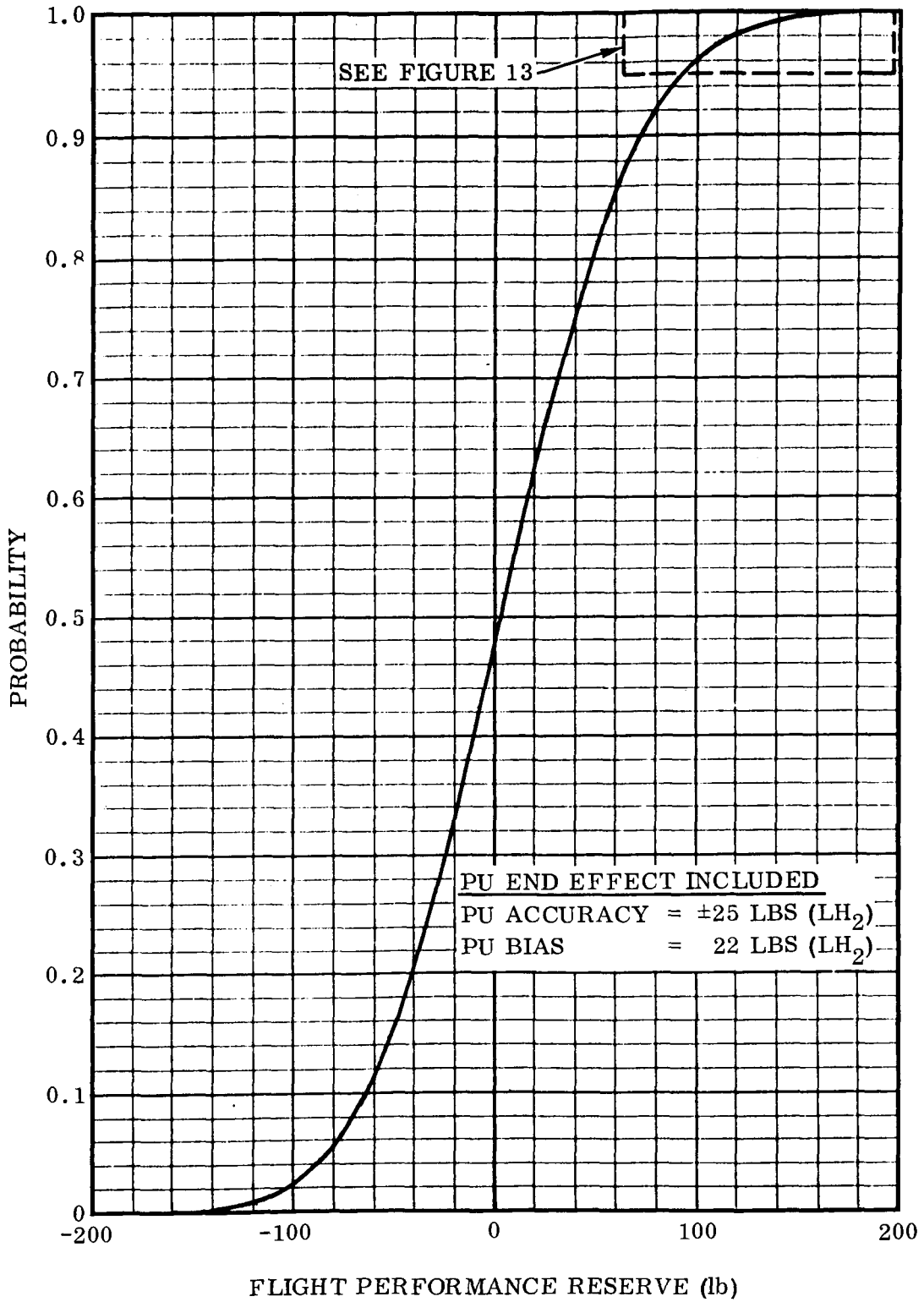Figure 11. FPR Frequency Function (PU End Effect Included)

SEE FIGURE 13

PU END EFFECT INCLUDED
PU ACCURACY = ±25 LBS (LH$_2$)
PU BIAS = 22 LBS (LH$_2$)

FLIGHT PERFORMANCE RESERVE (lb)
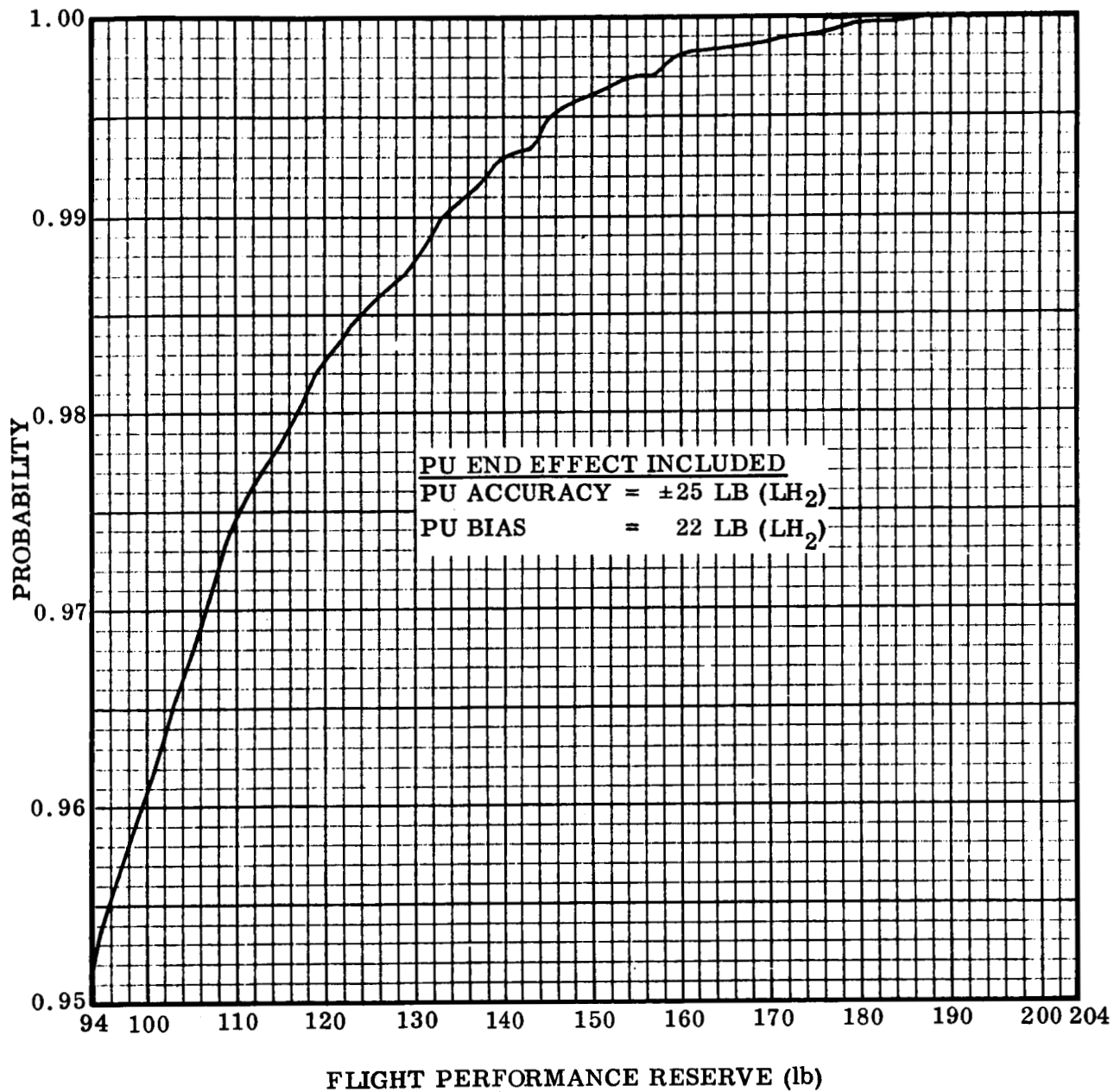
PROBABILITY

Figure 12. FPR Probability Function (PU End Effect Included)

Figure 13. FPR Probability Function Segment (PU End Effect Included)

$$HBP + (CPUB-SUBBIAS) + R_1 \qquad\qquad (A-1)$$

pounds of LH_2 available (with a minimum of HBP).

Now, for an average of VALVLAG seconds the mixture ratio is (PUSET+MAXSET)/2:1 and for the remainder of the burn, the ratio is MAXSET:1.

The average liquid oxygen flow rate is

$$(MR/MR+1) \; (\dot\omega_1 + \dot\omega_2)$$

Therefore, the total remaining burn time is approximately

$$\{LBP \; (MR+1)\}/\{(\dot\omega_1 + \dot\omega_2) \; MR\} \text{ seconds}.$$

Consequently, the average mixture ratio after liquid oxygen probe uncovery, $\overline{MR}$, is

$$\overline{MR} = \frac{(VALVLAG)(MR)(\dot\omega_1 + \dot\omega_2)}{LBP \, (MR+1)} \left\{ \frac{PUSET + MAXSET}{2} \right\}$$

$$+ \left\{ 1 - \frac{VALVLAG \, (MR) \, (\dot\omega_1 + \dot\omega_2)}{LBP \, (MR+1)} \right\} \cdot MAXSET$$

or

$$\overline{MR} = \frac{MR \, (\dot\omega_1 + \dot\omega_2) \; VALVLAG \; (PUSET-MAXSET)}{2 \; LBP \; (MR+1)} + MAXSET$$

The units of LH_2 needed at this mixture ratio for liquid oxygen depletion are

$$LBP/\overline{MR} \text{ pounds} \qquad\qquad (A-2)$$

Therefore, the LH_2 residual is the difference between the available and needed LH_2 (Equations A-1 and A-2)

$$LH_2 \text{ residual} = HBP + (CPUB-SUBBIAS) + R_1 - LBP/\overline{MR}$$

But, nominally, there are CPUB pounds of LH_2 left.

So,

$$d\alpha_{14_8} = HPB + R_1 - SUBBIAS - LBP/\overline{MR} \qquad\qquad (A-3)$$

If

$$d\alpha_{14_8} < 0$$

then

$$d\alpha_{14_8} = - d\alpha_{14_8} \times \overline{MR}$$

Similarly, for the situation of LH_2 probe uncovery there are HBP pounds of LH_2 available.

The LO_2 weight at uncovery is

$$LBP + (SUBBIAS-CPUB) \; PUSET + R_2 \quad \text{(with a minimum of LBP)} \qquad \text{(A-4)}$$

where R_2 is a random liquid oxygen uncertainty variate.

Again, for VALVLAG seconds, the mixture ratio is (PUSET-MINSET)/2:1 and then it is MINSET:1.

Since the average LH_2 flow rate is

$$\frac{1}{MR+1} \; (\dot\omega_1 + \dot\omega_2)$$

the total remaining burn time is approximately

$$\frac{HBP(MR+1)}{\dot\omega_1 + \dot\omega_2} \quad \text{seconds.}$$

Therefore, the average mixture ratio after LH_2 probe uncovery is

$$\overline{\overline{MR}} = \frac{(\dot\omega_1 + \dot\omega_2) \; VALVLAG \; (PUSET-MINSET)}{2 \; HBP \; (MR+1) \cdot} + MINSET$$

this necessitates the consumption of

$$\overline{\overline{MR}} \times HBP \qquad \text{(A-5)}$$

pounds of LO_2 for LH_2 depletion.

Consequently, the LO_2 residual is the difference between relation A-4 and A-5.

$$d\alpha_{14_8} = \text{LBP} + (\text{SUBBIAS-CPUB}) \times \text{PUSET+R}_2 - \overline{\overline{\text{MR}}} \times \text{HBP} \qquad \text{(A-6)}$$

Also, if

$$d\alpha_{14_8} < 0$$

then

$$d\alpha_{14_8} = -d\alpha_{14_8} \cdot \frac{1}{\overline{\overline{\text{MR}}}} \qquad \text{(A-7)}$$

Important input values which have been used in generating the preceding data are.

HBP (Hydrogen Below Probe)	= 261* pounds
LBP (LOX Below Probe)	= 1001* pounds
HBPDIS (HBP Dispersion)	= ± 7 pounds
LBPSID (LBP Dispersion)	= ±34 pounds
VALVLAG (PU Valve Lag Time)	= 5 seconds
MAXSET (Mixture Ratio at LO_2 Rich Stop)	= 5.55
MINSET (Mixture Ratio at LH_2 Rich Stop)	= 4.39
PUSET (Null Mixture Ratio)	= 5.00

*Adjusted for non-alignment of vehicle center line with thrust vector at probe uncovering. Without adjustment, these numbers are HPB = 267 and LBB = 1029.